

See discussions, stats, and author profiles for this publication at: <https://www.researchgate.net/publication/5673301>

Spin States at a Tipping Point: What Determines the $d z^2$ Ground State of Nickel(III) Tetra(*t* butyl)porphyrin Dicyanide?

ARTICLE *in* THE JOURNAL OF PHYSICAL CHEMISTRY B · FEBRUARY 2008

Impact Factor: 3.3 · DOI: 10.1021/jp709980y · Source: PubMed

CITATIONS

10

READS

19

3 AUTHORS, INCLUDING:



Jeanet Conradie

University of the Free State

142 PUBLICATIONS 1,854 CITATIONS

SEE PROFILE



Abhik Ghosh

UiT - The Arctic University of Norway

187 PUBLICATIONS 5,401 CITATIONS

SEE PROFILE

Spin States at a Tipping Point: What Determines the $d_{z^2}^1$ Ground State of Nickel(III) Tetra(*t*-butyl)porphyrin Dicyanide?

Jeanet Conradie,^{†,‡} Tebikie Wondimagegn,[†] and Abhik Ghosh^{*,†}

Department of Chemistry and Center for Theoretical and Computational Chemistry, University of Tromsø, N-9037 Tromsø, Norway, and Department of Chemistry, University of the Free State, 9300 Bloemfontein, Republic of South Africa

Received: October 13, 2007; In Final Form: November 8, 2007

Density functional theory (DFT) calculations, regardless of the exchange-correlation functional, have long failed to reproduce the observed $d_{z^2}^1$ ground state of the $[\text{Ni}^{\text{III}}(\text{T}^t\text{BuP})(\text{CN})_2]^-$ anion (where T^{*t*}BuP is the strongly ruffled tetra(*t*-butyl)porphyrin ligand), predicting instead a $d_{x^2-y^2}^1$ ground state. Normally, such failures are associated with DFT calculations on spin states of different multiplicity, which is not the case here. The calculations reported here strongly suggest that the problem does not lie with DFT. Instead environmental factors need to be taken into account, such as counterions and solvents. Counterions such as K^+ placed against the cyanide nitrogens and polar solvents both result in a $d_{z^2}^1$ ground state, thus finally reconciling theory and experiment.

The unusual chemistry of the nickel tetrapyrrole cofactor F₄₃₀ in the catalytic cycle of the enzyme methylcoenzyme M reductase (MCR),¹ which catalyzes the last step of biological methanogenesis, has long inspired the study of synthetic nickel porphyrins and hydroporphyrins.² Of particular interest has been the role of macrocycle conformation, planarity or otherwise, which has led to the synthesis of numerous nonplanar porphyrin derivatives.² Another line of inquiry has focused on the oxidative chemistry of nickel porphyrins, where, in a seminal contribution, Bocian and co-workers showed that, depending on the axial ligands, six-coordinate nickel(III) porphyrins exhibit one of two different d electron configurations.³ Thus, electron paramagnetic resonance (EPR) studies (*g* values and hyperfine parameters) have shown the two complexes $[\text{Ni}^{\text{III}}(\text{TPP})(\text{py})_2]^+$ ($g_{\perp} > g_{\parallel}$) and $[\text{Ni}^{\text{III}}(\text{TPP})(\text{CN})_2]^-$ ($g_{\perp} < g_{\parallel}$) to have a $d_{z^2}^1$ and a $d_{x^2-y^2}^1$ ground state, respectively.³ These electronic configurations are readily understood in terms of qualitative ligand field theory considerations: the unpaired electron in these low-spin d^7 species prefers to be in the d orbital that is less destabilized by the ligand field. Density functional theory (DFT) (PW91/STO-TZP) calculations readily confirmed these assignments, correctly predicting the appropriate ground states for pyridine and cyanide axial ligands.⁴

In 2002, however, Fajer and co-workers reported another development in this field that has resisted theoretical modeling until now.⁵ These authors showed that, for the strongly nonplanar tetra(*t*-butyl)porphyrin (T^{*t*}BuP) ligand, both the $\text{Ni}^{\text{III}}(\text{py})_2$ and the $\text{Ni}^{\text{III}}(\text{CN})_2$ complexes (in CH_2Cl_2) exhibit $d_{z^2}^1$ ground states. In the latter complex, the contracted core of the highly ruffled porphyrin apparently destabilizes the $d_{x^2-y^2}$ orbital so much that the unpaired electron prefers to occupy the $d_{z^2}^1$

orbital and thereby interact with the exceedingly strong-field cyanide ligands. Surprisingly, in contrast to this experimental finding, *every* commonly used DFT functional predicts a $d_{x^2-y^2}^1$ ground state for $[\text{Ni}^{\text{III}}(\text{T}^t\text{BuP})(\text{CN})_2]^-$. What might account for this failure? We report here a set of DFT calculations that afford a plausible solution to this conundrum.^{6,7}

Figure 1 depicts selected results for the $d_{z^2}^1$ and $d_{x^2-y^2}^1$ states of $[\text{Ni}^{\text{III}}(\text{T}^t\text{BuP})(\text{CN})_2]^-$, optimized with OLYP^{8,9}/STO-TZP and a D_{2d} symmetry constraint. Also shown for comparison are optimized structures of $\text{Ni}^{\text{II}}\text{T}^t\text{BuP}^{10}$ and $\text{Cu}^{\text{II}}\text{T}^t\text{BuP}$, both of which were found to exhibit purely ruffled, D_{2d} minima. Observe that the $d_{x^2-y^2}^1$ state has substantially longer metal–nitrogen distances (like $\text{Cu}^{\text{II}}\text{T}^t\text{BuP}$) and is also less ruffled (as measured by the ruffling dihedral angle), relative to the Ni(II) and Ni(III) $d_{z^2}^1$ states. For OLYP-optimized geometries, the energy margins by which the $d_{x^2-y^2}^1$ state is (incorrectly) favored over the $d_{z^2}^1$ state are 1.6 (OLYP), 3.0 (PW91),¹¹ 3.7 (OPBE),^{8,12} 1.4 (BLYP),^{9,13} 0.5 (B3LYP),¹⁴ and 1.2 (B3LYP*)^{14a,15} kcal/mol, depending on the functional. Of course, an occasional failure of DFT to yield the correct spin state for a transition metal complex is not surprising, especially where the energy differences involved are only a few kilocalories per mole; however, such failures typically involve spin states of different multiplicities.^{16,17} In this case, however, we are comparing two electronic states (i.e., the $d_{z^2}^1$ and $d_{x^2-y^2}^1$ states, both doublets) of the same multiplicity, and it is puzzling indeed why *every* commonly used exchange-correlation functional should predict the wrong ground state.

We were stumped by this conundrum for several years until it occurred to us that the problem might lie not with DFT, but with our isolated-ion model. The obvious way to refine our model of $\text{K}[\text{Ni}^{\text{III}}(\text{T}^t\text{BuP})(\text{CN})_2]$ in solution was to consider environmental effects such as counterions and the solvent. In one D_{2d} model, $\{\text{K}_2[\text{Ni}^{\text{III}}(\text{T}^t\text{BuP})(\text{CN})_2]\}^+$, we placed a pair of

* Corresponding author. E-mail: abhik@chem.uit.no.

[†] University of Tromsø.

[‡] University of the Free State.

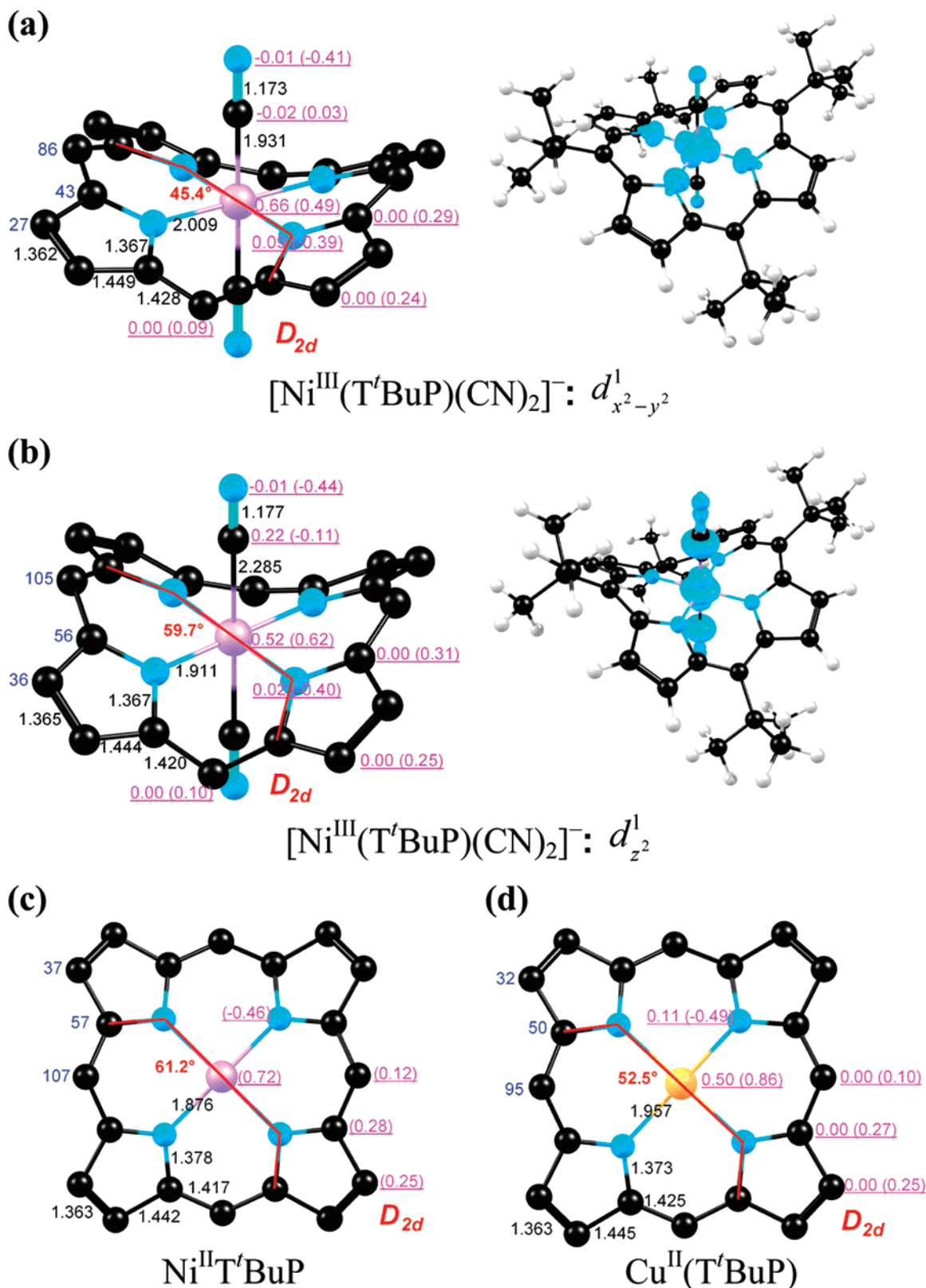


Figure 1. Selected distances (Å, in black), Mulliken spin populations (in magenta), charges (in magenta, within parentheses), out-of-plane displacements (pm, in blue), and the ruffling dihedral angle (deg, in red) for the OLYP/TZP-optimized structures of some T'BuP derivatives. Selected spin density profiles are plotted in cyan. Color code for atoms: C (black), N (cyan), H (ivory), Ni (lilac), and Cu (orange).

K^+ ions against the cyanide nitrogens on the S_4 axis. In another D_{2d} model, $\{\text{K}_2\text{Cl}_2[\text{Ni}^{\text{III}}(\text{T}'\text{BuP})(\text{CN})_2]\}^-$, we placed a pair of K^+Cl^- ion pairs against the cyanide nitrogens and along the S_4 axis, i.e., resulting in a $\text{C}\equiv\text{N}\cdots\text{K}\cdots\text{Cl}$ arrangement on each side. The KCl groups are intended to mimic the effect of crown ether-

complexed K^+ ions, which are the likely counterions in the experimental studies.⁵ The chloride ions are assumed to mute the effect of bare K^+ ions somewhat, as a crown ether would. The advantage of the KCl groups, as opposed to crown ethers, is of course that the former preserve the full D_{2d} symmetry of

TABLE 1: OLYP/TZP Relative Energies (kcal/mol) of the $d_{z^2}^1$ (Chosen as Zero Level) and $d_{x^2-y^2}^1$ States of $[\text{Ni}^{\text{III}}(\text{T}^{\text{t}}\text{BuP})(\text{CN})_2]^-$, $\{\text{K}_2[\text{Ni}^{\text{III}}(\text{T}^{\text{t}}\text{BuP})(\text{CN})_2]\}^+$, and $\{\text{K}_2\text{Cl}_2[\text{Ni}^{\text{III}}(\text{T}^{\text{t}}\text{BuP})(\text{CN})_2]\}^-$ as a Function of Different Solvents, Described by the COSMO Model

type of calculation:	ϵ	geometry optimization throughout		geometry optimization in vacuum; single-point cosmo			
		$[\text{Ni}^{\text{III}}(\text{T}^{\text{t}}\text{BuP})(\text{CN})_2]^-$		$\{\text{K}_2[\text{Ni}^{\text{III}}(\text{T}^{\text{t}}\text{BuP})(\text{CN})_2]\}^+$		$\{\text{K}_2\text{Cl}_2[\text{Ni}^{\text{III}}(\text{T}^{\text{t}}\text{BuP})(\text{CN})_2]\}^-$ single-point COSMO	
		$d_{x^2-y^2}^1$	$d_{z^2}^1$	$d_{x^2-y^2}^1$	$d_{z^2}^1$	$d_{x^2-y^2}^1$	$d_{z^2}^1$
vacuum	1	-1.6	0.0	3.7	0.0	0.0	0.0
CHCl_3	4.8	-0.5	0.0	3.7	0.0	1.6	0.0
CH_2Cl_2	8.9	0.2	0.0	3.6	0.0	2.5	0.0
CH_3OH	32.6	2.1	0.0	3.5	0.0	4.8	0.0
DMSO	46.7	2.8	0.0	5.3	0.0	3.0	0.0

the problem. Finally, as shown in Figure 2, we let a pair of methanol molecules hydrogen-bond to the cyanide nitrogens. All these models were fully optimized (with OLYP/TZP and an appropriate symmetry constraint), and we were pleased to find that each exhibits a $d_{z^2}^1$ spin state. Subsequently, we attempted to account for solvation effects using Conductor-like Screening Model (COSMO)¹⁸ calculations on $[\text{Ni}^{\text{III}}(\text{T}^{\text{t}}\text{BuP})(\text{CN})_2]^-$, $\{\text{K}_2[\text{Ni}^{\text{III}}(\text{T}^{\text{t}}\text{BuP})(\text{CN})_2]\}^+$, and $\{\text{K}_2\text{Cl}_2[\text{Ni}^{\text{III}}(\text{T}^{\text{t}}\text{BuP})(\text{CN})_2]\}^-$ for chloroform, dichloromethane, methanol, and DMSO, and, as shown in Table 1, the results indicate that increasing polarity of the solvent stabilizes the $d_{z^2}^1$ state relative to the $d_{x^2-y^2}^1$ state.

The relative invariance of the above results for different functionals (the somewhat unnecessary details are not presented here) suggests that we have successfully captured the essence of the factors determining the spin-state energetics of $\text{K}[\text{Ni}^{\text{III}}(\text{T}^{\text{t}}\text{BuP})(\text{CN})_2]$ in dichloromethane solution. The strong-field cyanide axial ligands and the strong equatorial $\text{T}^{\text{t}}\text{BuP}$ ligand result in near-degenerate $d_{z^2}^1$ and $d_{x^2-y^2}^1$ states. Such a near-degeneracy, common for $\text{Fe}(\text{II})$ and $\text{Fe}(\text{III})$ complexes,¹⁹ is unprecedented for $\text{Ni}(\text{III})$.²⁰ However, according to the present study, the $\text{T}^{\text{t}}\text{BuP}$ ligand does not by itself lead to a $d_{z^2}^1$ state,

but environmental effects, most likely K^+ counterions, aided by the solvent, are what ultimately tip the balance in favor of the observed $d_{z^2}^1$ ground state.

To understand why the $d_{z^2}^1$ state is preferentially stabilized by K^+ ions (or by a hydrogen bond donor such as methanol), we examined the Mulliken charges and spin populations of the various models mentioned above; these are summarized in Figure 2. Although we cannot definitively tell why one spin state is stabilized over the other, we have identified a possible reason: the Mulliken charge on each cyanide carbon is about 0.15e higher (i.e., significantly more positive) for the $d_{x^2-y^2}^1$ state than for the $d_{z^2}^1$ state, which suggests that the latter state should be more stabilized by positive ions interacting directly with the cyanide nitrogens (it may be recalled that electrostatic forces are long-range relative to atomic and molecular dimensions).

Overall, this study enlarges our perspective of the electronic-structural diversity of $\text{Ni}(\text{III})$ complexes and intermediates, biological or otherwise. Recently, two groups have furnished EPR characterization of an inactivated $d_{x^2-y^2}^1$ Ni^{III} -alkyl-MCR intermediate.²¹ In addition, Hoffmann and co-workers have reported ENDOR characterization of what is believed to be the actual Ni^{III} -methyl-MCR catalytic intermediate.²² All of these studies nicely confirm our theoretical DFT (PW91) prediction of the possible existence of just such a species.²³ Overall, studies on F_{430} , MCR, and model complexes have shown that two different spin states are observed for octahedral $\text{Ni}(\text{III})$ species; which one happens to be the ground state for a given complex depends largely on the relative strengths of the equatorial and axial ligands. This study provides a remarkable example where the axial ligand strength depends not only on the ligand itself but also on environmental factors. Indeed, counterions appear to be the ultimate determinant of the observed ground state of the $\text{Ni}(\text{III})$ porphyrin intermediate that is the subject of this study.

Acknowledgment. This work was supported by the Research Council of Norway (A.G.) and the Central Research Fund of the University of the Free State (J.C.).

Supporting Information Available: Optimized Cartesian coordinates for selected systems (9 pages). This material is available free of charge via the Internet at <http://pubs.acs.org>.

References and Notes

- (1) (a) Shima, S.; Thauer, R. K. *Curr. Opin. Microbiol.* **2005**, *8*, 643–648. (b) Ragsdale, S. W. In *The Porphyrin Handbook*; Kadish, K. M., Smith, K. M., Guillard, R., Eds.; Academic (Elsevier): San Diego, CA, 2003; Vol. 11, Chapter 67, pp 205–228. (c) Ghosh, A.; Wondimagegn, T.; Ryeng, H. *Curr. Opin. Chem. Biol.* **2002**, *5*, 744–750. (d) Telser, J. *Struct. Bonding* **1998**, *91*, 31.

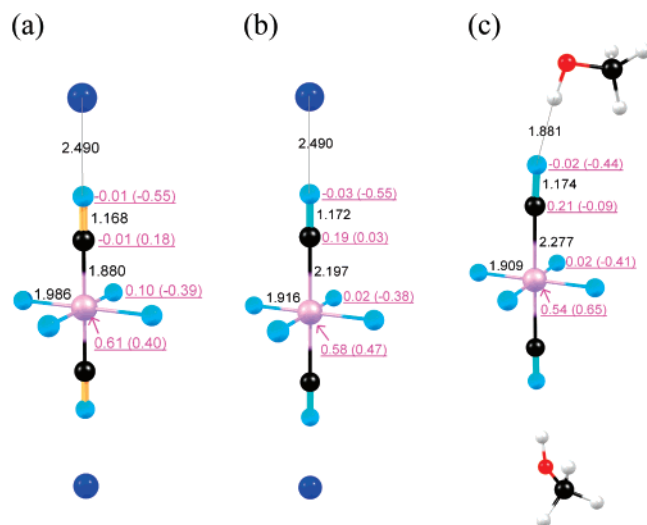


Figure 2. Selected results on modeling environmental effects on $[\text{Ni}^{\text{III}}(\text{T}^{\text{t}}\text{BuP})(\text{CN})_2]^-$: (a) the 2B_1 (D_{2d}) $d_{x^2-y^2}^1$ spin state of $\{\text{K}_2[\text{Ni}^{\text{III}}(\text{T}^{\text{t}}\text{BuP})(\text{CN})_2]\}^+$; (b) the 2A_1 (D_{2d}) $d_{z^2}^1$ spin state of $\{\text{K}_2[\text{Ni}^{\text{III}}(\text{T}^{\text{t}}\text{BuP})(\text{CN})_2]\}^+$; and (c) the 2A_1 (C_2) $d_{z^2}^1$ spin state of $[\text{Ni}^{\text{III}}(\text{T}^{\text{t}}\text{BuP})(\text{CN})_2]^- \cdot 2\text{CH}_3\text{OH}$. For a and b, the $\text{N} \cdots \text{K}$ distances were constrained to 2.49 Å (this is the mean of the distances that would be obtained if the dipotassium complex were fully optimized for the two spin states), with all other internal coordinates being optimized. For c, the whole structure was optimized. Color code for atoms: same as in Figure 1; K (blue). Selected distances are indicated in black, and spin populations (charges in parentheses) are shown in magenta. These results may be compared with those shown in Figure 1(a,b) for the naked $[\text{Ni}^{\text{III}}(\text{T}^{\text{t}}\text{BuP})(\text{CN})_2]^-$ anion.

- (2) (a) Shelnutt, J. A.; Song, X. Z.; Ma, J. G.; Jia, S. L.; Jentzen, W.; Medforth, C. J. *Chem. Soc. Rev.* **1998**, 27, 31–41. (b) Senge, M. O. *Chem. Commun.* **2006**, 243–256.
- (3) Seth, J.; Palaniappan, V.; Bocian, D. F. *Inorg. Chem.* **1995**, 34, 2201–2206.
- (4) Ghosh, A.; Wondimagegn, T.; Gonzalez, E.; Halvorsen, I. J. *Inorg. Biochem.* **2000**, 78, 79–82.
- (5) Renner, M. W.; Barkigia, K. M.; Melamed, D.; Gisselbrecht, J. P.; Nelson, N. Y.; Smith, K. M.; Fajer, J. *Res. Chem. Intermed.* **2002**, 28, 741–759.
- (6) Throughout this study, we used all-electron Slater-type triple- ζ plus polarization (TZP) basis sets, a variety of exchange-correlation functionals, and a fine mesh for numerical integration of matrix elements, all as implemented in the ADF 2006 program system.
- (7) For reviews on quantum chemical studies of transition metal porphyrins, see: (a) Ghosh, A.; Steene, E. *J. Biol. Inorg. Chem.* **2001**, 6, 739–752. (b) Ghosh, A. In *The Porphyrin Handbook*; Kadish, K. M., Smith, K. M., Guillard, R., Eds.; Academic (Elsevier): San Diego, CA, 2000; Vol. 7, Chapter 47, pp 1–38.
- (8) Handy, N. C.; Cohen, A. J. *Mol. Phys.* **2001**, 99, 403–412.
- (9) Lee, C.; Yang, W.; Parr, R. G. *Phys. Rev.* **1988**, B37, 785–789.
- (10) Song, X.-Z.; Jentzen, W.; Jaquinod, L.; Khoury, R. G.; Medforth, C. J.; Jia, S.-L.; Ma, J.-G.; Smith, K. M.; Shelnutt, J. A. *Inorg. Chem.* **1998**, 37, 2117–2128.
- (11) Perdew, J. P.; Chevary, J. A.; Vosko, S. H.; Jackson, K. A.; Perderson, M. R.; Singh, D. J.; Fiolhais, C. *Phys. Rev. B* **1992**, 46, 6671–6687. Erratum: Perdew, J. P.; Chevary, J. A.; Vosko, S. H.; Jackson, K. A.; Perderson, M. R.; Singh, D. J.; Fiolhais, C. *Phys. Rev. B* **1993**, 48, 4978.
- (12) (a) Perdew, J. P.; Burke, K.; Ernzerhof, M. *Phys. Rev. Lett.* **1996**, 77, 3865–3868. (b) Perdew, J. P.; Burke, K.; Ernzerhof, M. *Phys. Rev. Lett.* **1997**, 78, 1396.
- (13) Becke, A. D. *Phys. Rev.* **1988**, A38, 3098.
- (14) (a) Watson, M. A.; Handy, N. C.; Cohen, A. J. *J. Chem. Phys.* **2003**, 119, 6475–6481. (b) Stephens, J.; Devlin, F. J.; Chabalowski, C. F.; Frisch, M. J. *J. Phys. Chem.* **1994**, 98, 11623–11627. (c) Hertwig, R. H.; Koch, W. *Chem. Phys. Lett.* **1997**, 268, 345–351.
- (15) Reiher, M.; Salomon, O.; Hess, B. A. *Theor. Chem. Acc.* **2001**, 107, 48.
- (16) Reviews on DFT calculations on transition metal spin-state energetics: (a) Ghosh, A.; Taylor, P. R. *Curr. Opin. Chem. Biol.* **2003**, 91, 113–124. (b) Ghosh, A. *J. Biol. Inorg. Chem.* **2006**, 11, 671–673.
- (17) Selected studies comparing the performance of different functionals vis-à-vis transition metal spin-state energetics: (a) Swart, M.; Groenhof, A. R.; Ehlers, A. W.; Lammertsma, K. *J. Phys. Chem. A* **2004**, 108, 5479–5483. (b) Swart, M.; Ehlers, A. W.; Lammertsma, K. *Mol. Phys.* **2004**, 102, 2467–2474. (c) Deeth, R. J.; Fey, N. J. *Comput. Chem.* **2004**, 25, 1840–1848. (d) Groenhof, A. R.; Swart, M.; Ehlers, A. W.; Lammertsma, K. *J. Phys. Chem. A* **2005**, 109, 3411–3417. (e) Daku, L. M. L.; Vargas, A.; Hauser, A.; Fouqueau, A.; Casida, M. E. *ChemPhysChem* **2005**, 6, 1393–1410. (f) Ganzenmuller, G.; Berkaine, N.; Fouqueau, A.; Casida, M. E.; Reiher, M. *J. Chem. Phys.* **2005**, 122, Art. No. 234321. (g) De Angelis, F.; Jin, N.; Car, R.; Groves, J. T. *Inorg. Chem.* **2006**, 45, 4268–4276. (h) Vargas, A.; Zerara, M.; Krausz, E.; Hauser, A.; Daku, L. M. L. *J. Chem. Theory Comput.* **2006**, 2, 1342–1359. (i) Rong, C. Y.; Lian, S. X.; Yin, D. L.; Shen, B.; Zhong, A. G.; Bartolotti, L.; Liu, S. B. *J. Chem. Phys.* **2006**, 125, Art. No. 174102. (j) Strickland, N.; Harvey, J. N. *J. Phys. Chem. B* **2007**, 111, 841–852.
- (18) (a) Klamt, A.; Schüürmann, G. *J. Chem. Soc., Perkin Trans.* **1993**, 2, 799–805. (b) Klamt, A. *J. Phys. Chem.* **1995**, 99, 2224–2235.
- (19) For a DFT study on a spin-crossover Fe complex, see: Conradie, J.; Ghosh, A. *J. Phys. Chem. B*, **2007**, 111, 12621–12624.
- (20) Review of Ni(III) and Ni(IV) complexes: Meyer, F.; Koslowski, H. In *Comprehensive Coordination Chemistry II*; McLeverty, J., Meyer, T. J., Eds.; Elsevier: Amsterdam, 2004; Vol. 6, Chapter 6.3, pp 252–275.
- (21) (a) Hinderberger, D.; Piskorski, R. R.; Goenrich, M.; Thauer, R. K.; Schweiger, A.; Harmer, J.; Jaun, B. *Angew. Chem., Int. Ed.* **2006**, 45, 3602–2607. (b) Yang, N.; Reiher, M.; Wang, M.; Harmer, J.; Duin, E. C. *J. Am. Chem. Soc.* **2007**, 129, 11028–11029.
- (22) Dey, M.; Telser, J.; Kunz, R. C.; Lees, N. S.; Ragsdale, S. W.; Hoffman, B. M. *J. Am. Chem. Soc.* **2007**, 129, 11030–11032.
- (23) Wondimagegn, T.; Ghosh, A. *J. Am. Chem. Soc.* **2001**, 123, 5680–5683.